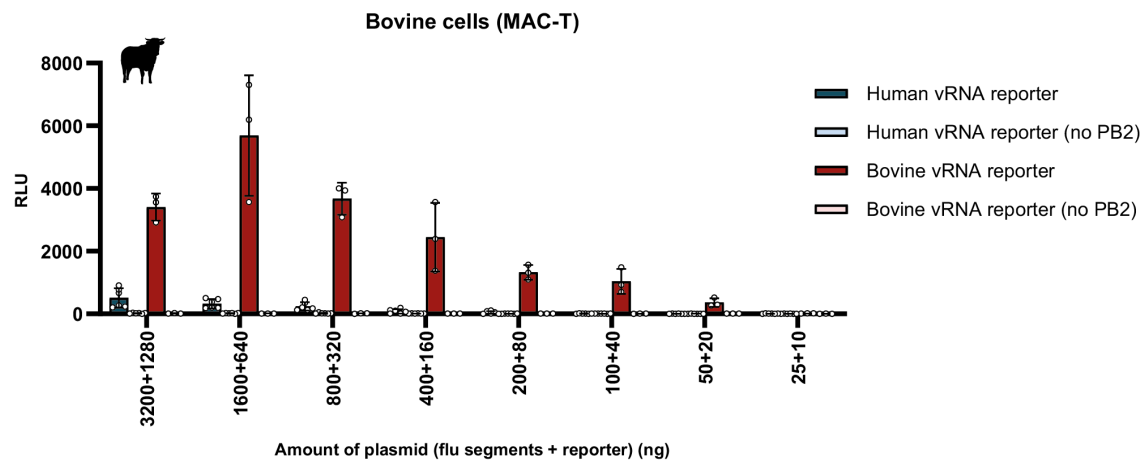
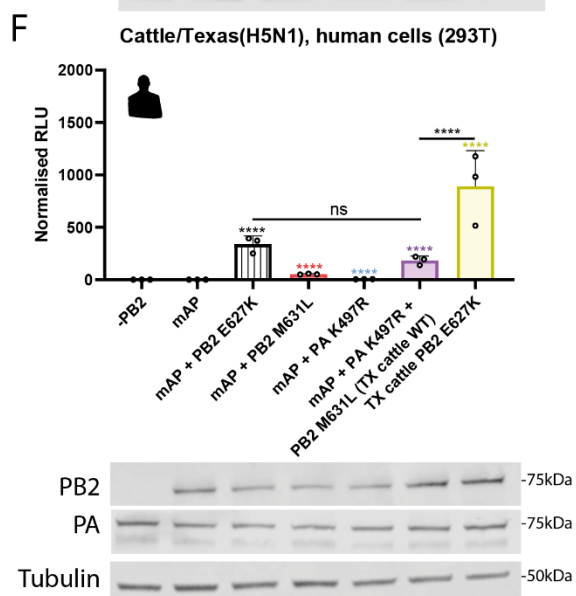
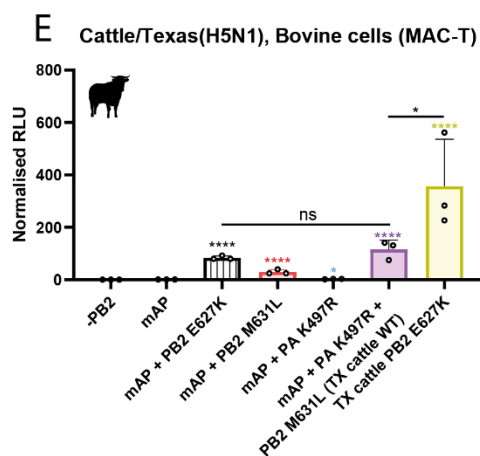
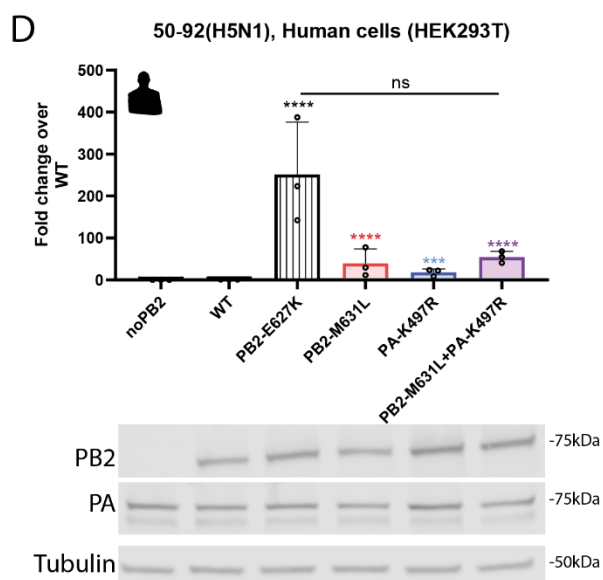
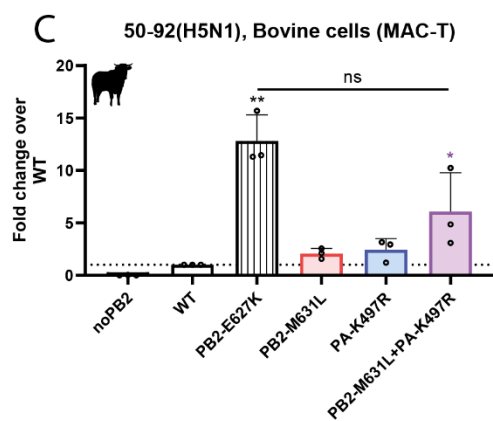
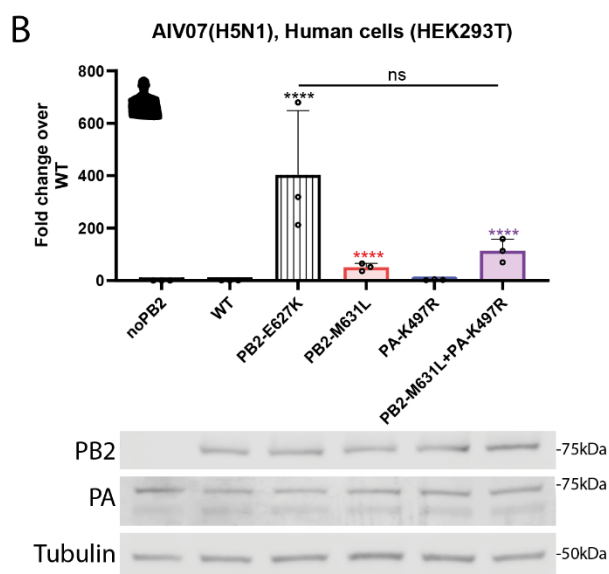
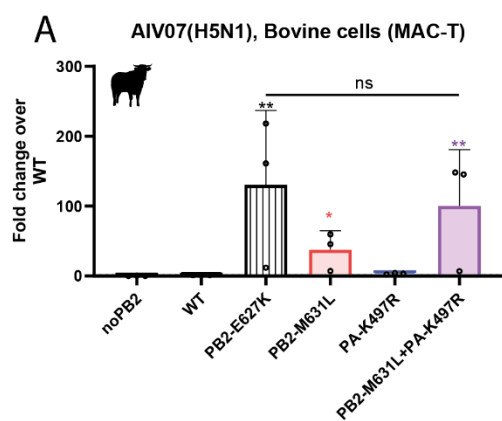


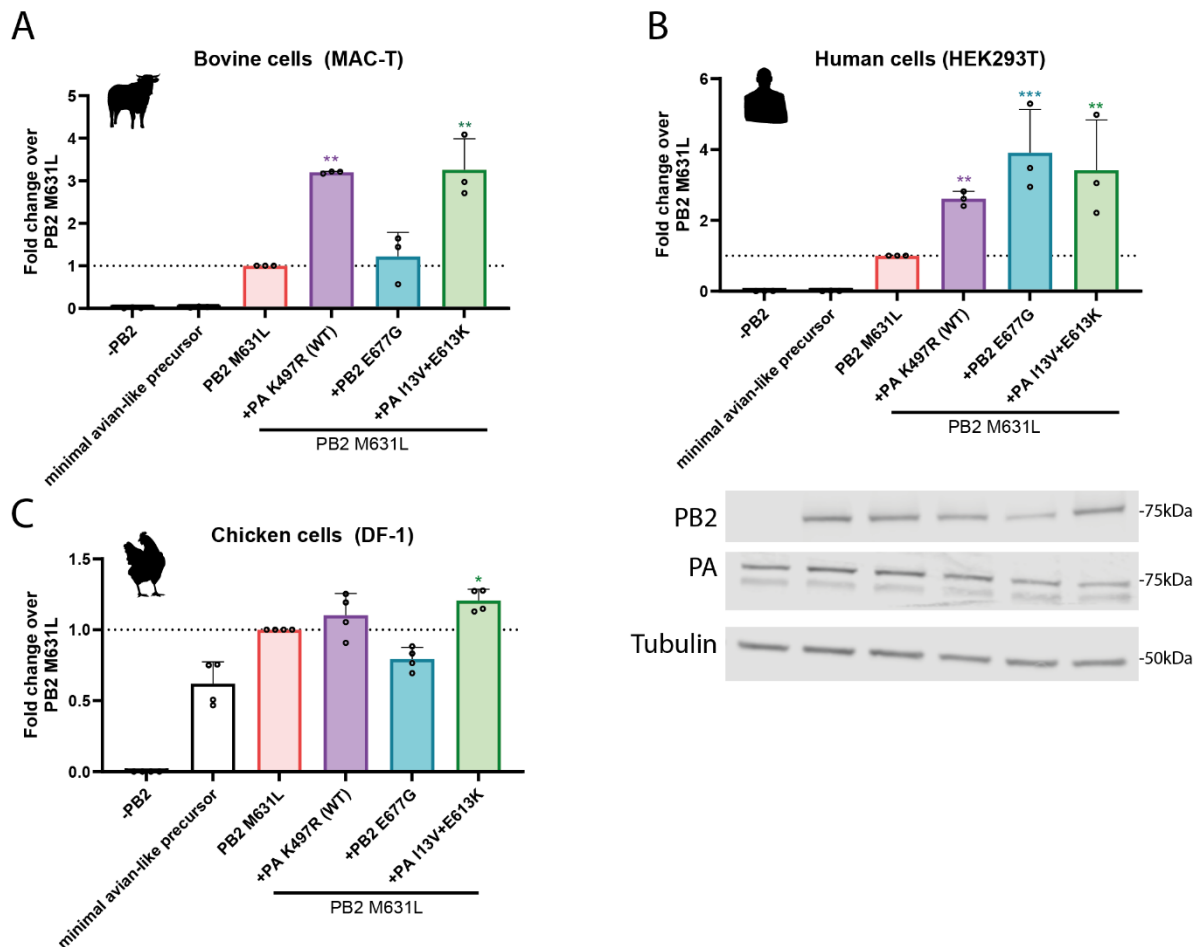
**Supplementary Figure S1. Phylogenetic analysis of bovine H5N1 viruses with key polymerase amino acid changes annotated.** Influenza sequences in the cattle outbreak, USA avian H5N1 sequences from 1st September 2023 – 31st March 2024 and A/Texas/37/2024 were concatenated and duplicates removed. The phylogenetic tree was created in IQTree2. Key polymerase mutations defining clades are highlighted.



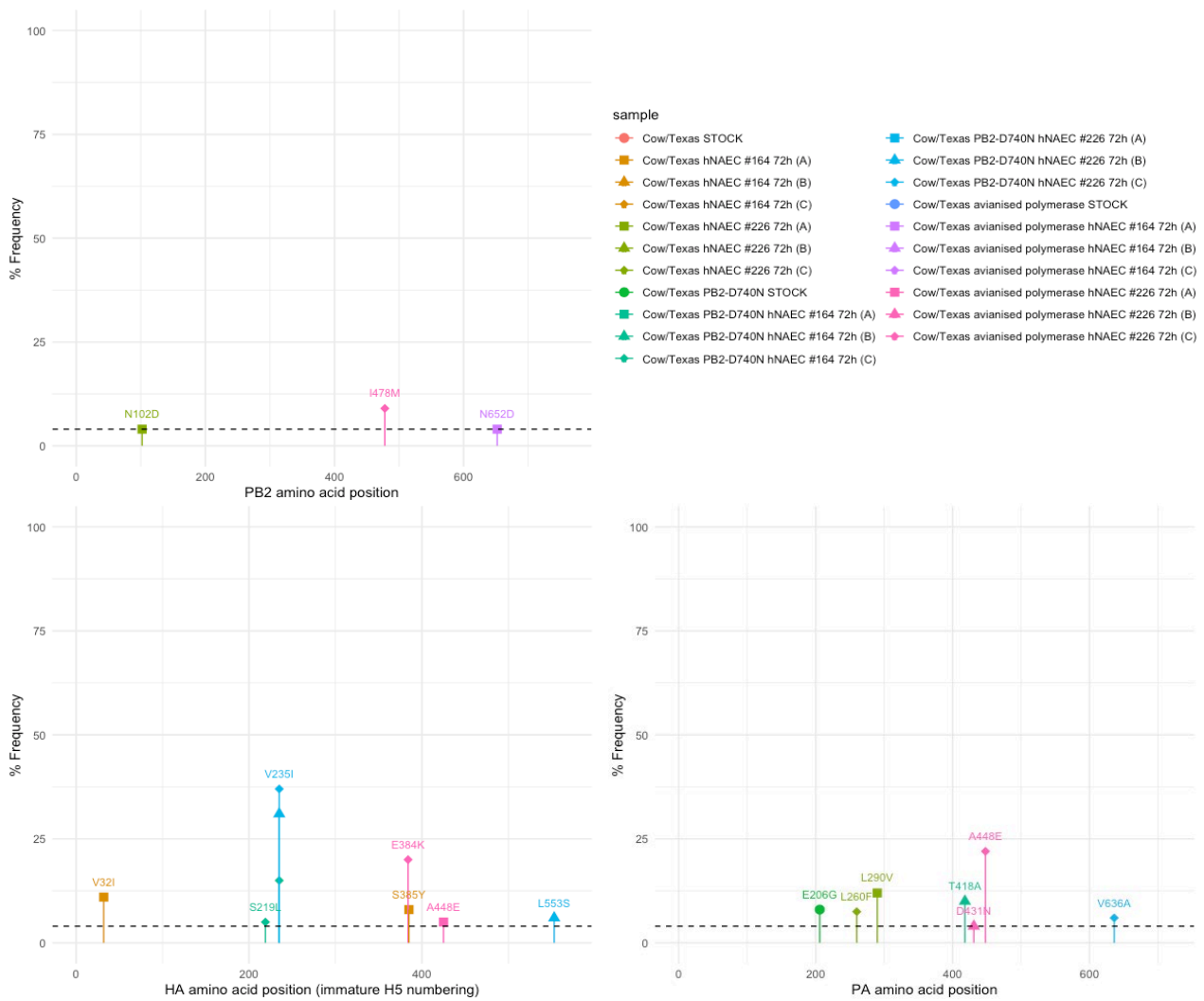
**Supplementary Figure S2. Generation and validation of a bovine cell-specific minireplicon reporter.** Validation of bovine-cell specific reporter vs human-cell specific reporter in bovine MAC-T cells. Data plotted as mean  $\pm$  SD. Minireplicon assay performed with either whole PR8 polymerase + NP, or PR8 polymerase + NP missing PB2.



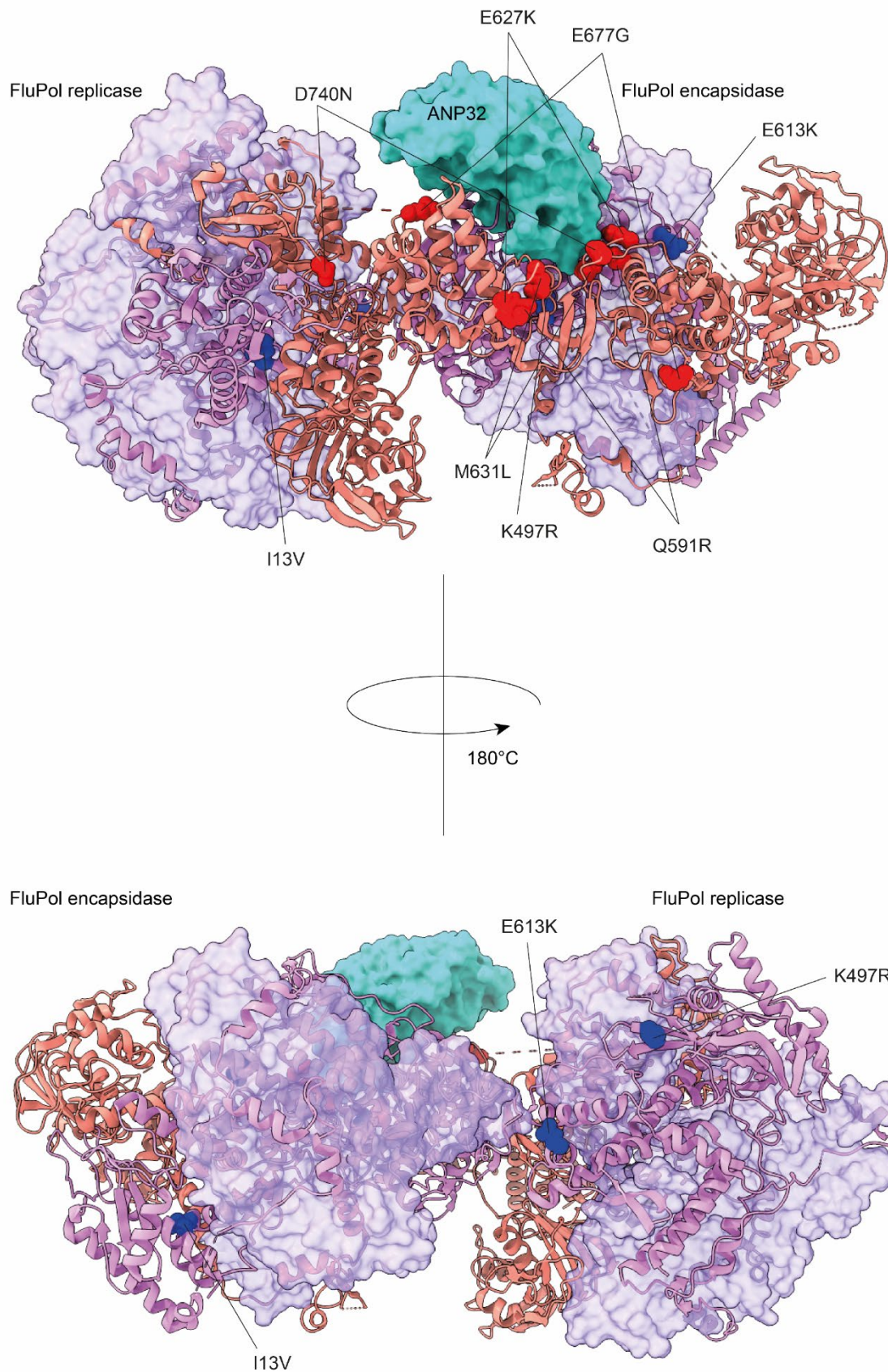
**Supplementary Figure S3. Polymerase mutations found in the major cattle clade also enhance mammalian cell polymerase activity in an unrelated genetic background.** Minigenome in (A,C,E) bovine MAC-T cells (B,D,F) human HEK293T, with mutant versions of a contemporary 2.3.4.4b UK H5N1 strain, A/chicken/England/053052/2021(H5N1) a.k.a. AIV07 (A,B) and the historic, non-goose/Guangdong H5N1 strain, A/turkey/England/50-92/1991(H5N1)(C,D) or of Cattle/Texas (E,F). Data normalised to WT. (B,D,F) Matched western blots showing expression of PB2 and PA. Data throughout plotted as the mean of N = 3 independent biological repeats. Data throughout plotted as mean + SD. Statistics throughout performed by one-way ANOVA with multiple comparisons comparing all data points, only comparisons between WT and mutants, and between PB2-E627K vs PB2-M631L+PA K497R marked on the figures. Log-normality determined by Shapiro-Wilk test and QQ plot. Significance shown by asterisks indicating: \*,  $0.05 \geq P > 0.01$ ; \*\*,  $0.01 \geq P > 0.001$ ; \*\*\*,  $0.001 \geq P > 0.0001$ ; \*\*\*\*,  $P \leq 0.0001$ .



**Supplementary Figure S4. Polymerase mutations on minor cattle branches also enhance polymerase activity in mammalian cells.** Minigenome in (A) bovine MAC-T cells (B) human HEK293T, (C) chicken DF-1 with mutant versions of cattle Texas. Data normalised to PB2 M631L. B) Expression of PB2 and PA from a matched western blot. Data throughout plotted as the mean of three independent biological repeats. Data throughout plotted as mean + SD. Statistics throughout performed by one-way ANOVA with multiple comparisons against PB2 M631L using log-transformed data. Log-normality determined by Shapiro-Wilk test and QQ plot. Significance shown by asterisks indicating: \*,  $0.05 \geq P > 0.01$ ; \*\*,  $0.01 \geq P > 0.001$ ; \*\*\*,  $0.001 \geq P > 0.0001$ ; \*\*\*\*,  $P \leq 0.0001$ .



**Supplementary Figure S5. Deep sequencing of viral populations from human nasal epithelial cells** Polymorphisms at >4% from the sequencing of inoculum and 72-hour samples taken from hNECs for the PB2, PA and HA genes. 3 technical replicates were sequenced for each virus for two donors at 72 hours post-infection. Only non-synonymous changes are shown. Limit of detection marked as a dashed line at 4%.



**Supplementary Figure S6: Extended structural mapping of cattle mutations onto the influenza virus polymerase.** H5N1 influenza A virus asymmetric polymerase dimer (PDB: 8R1J) showing human ANP32B in cyan, PB1 in purple, PB2 in salmon and PA as



ribbon representation in violet. The H5N1 cattle PA substitutions sites (13, 497, 613) are highlighted in blue and PB2 substitutions (591, 627, 631, 677, 740) are highlighted in red.